Electric field and temperature scaling of polarization reversal in silicon doped hafnium oxide ferroelectric thin films

Dayu Zhou,[a,b,*] Yan Guan,[a] Melvin M. Vopson,[c,+] Jin Xu,[d] Hailong Liang,[a] Fei Cao,[f] Xianlin Dong,[f] Tony Schenk,[e] and Uwe Schroeder[e]

[a]*Key Laboratory of Materials Modification by Laser, Ion, and Electron Beams (Ministry of Education), School of Materials Science and Engineering, Dalian University of Technology, Dalian 116024, China*

[b]*State Key Laboratory of Electronic Thin Films and Integrated Devices, University of Electronic Science and Technology of China, Chengdu 610054, China*

[c]*University of Portsmouth, Faculty of Science, SEES, Burnaby Building, Portsmouth PO1 3QL, UK*

[d]*Department of Electronic Engineering, Dalian Neusoft University of Information, Dalian 116023, China*

[f]*Key Laboratory of Inorganic Functional Materials and Devices, Shanghai Institute of Ceramics, Chinese Academy of Sciences, Shanghai 200050, China*

[e]*Namlab gGmbH/TU Dresden, Noethnitzer Strasse 64, 01187 Dresden, Germany*

[*] Corresponding author. Tel./fax: +86 411 84708206; E-mail address: zhoudayu@dlut.edu.cn
[+] Formerly known as Vopsaroiu

Abstract—HfO_2-based binary lead-free ferroelectrics show promising properties for non-volatile memory applications, providing that their polarization reversal behavior is fully understood. In this work, temperature-dependent polarization hysteresis measured over a wide applied field range has been investigated for Si-doped HfO_2 ferroelectric thin films. Our study indicates that in the low and medium electric field regimes ($E <$ twofold coercive field, $2E_c$), the reversal process is dominated by the thermal activation on domain wall motion and domain nucleation; while in the high-field regime ($E > 2E_c$), a non-equilibrium nucleation-limited-switching mechanism dominates the reversal process. The optimum field for ferroelectric random access memory (FeRAM) applications was determined to be around 2.0 MV/cm, which translates into a 2.0 V potential applied across the 10 nm thick films.

Keywords: Hafnium oxide; Ferroelectric; Domain switching; Temperature dependence; Reliability

1. Introduction

Recent studies show that pronounced ferroelectricity can be induced in hafnium oxide thin films when incorporated with various dopants (Si, Al, Y, Gd, La, and Sr) and annealed under certain conditions. The impacts of dopant type and concentration on the ferroelectric switching properties have been reviewed by Schroeder et al [1]. Furthermore, ferroelectricity can also be achieved in HfO_2-ZrO_2 solid-solution [2]. Apart from macroscopic polarization/strain hysteresis measurements and micro-structural analyses of the phase transition, conclusive evidences for the existence

of intrinsic ferroic behavior have also been provided by mesoscopic piezoresponse force microscopy (PFM) experiments [3] and first principles calculation [4-6].

Non-volatile ferroelectric memory will be one of the most attractive applications for this new type of lead-free and CMOS process compatible binary oxide ferroelectric material with comparatively low dielectric constant. When using it to replace conventional perovskite structure oxides, e.g. $Pb(Zr,Ti)O_3$ (PZT), a number of current integration and scaling issues in ferroelectric memory development can be eliminated [7]. Recent report of ferroelectric field effect transistors (FeFET) fabricated using Si-doped HfO_2 ($Si:HfO_2$) in 28 nm technology has evidenced this expectation [8].

The operation principle of nonvolatile ferroelectric memories is based on irreversible polarization reversal in ferroelectric thin films. A wealth of studies have shown that the polarization switching behavior of ferroelectrics depends strongly on material candidates, internal defects, interface properties, and external loads (i.e. electric field, temperature, and stress) [9, 10]. For instance, PZT displays higher switchable polarization than $SrBi_2Ta_2O_9$ (SBT), but suffers severe fatigue if no oxide electrodes are used; while SBT films sandwiched between two platinum electrodes are known as “fatigue-free” [11, 12]. An insufficient applied field will lead to a sub-loop, and the resultant incomplete writing should be avoided in ferroelectric random access memories (FeRAMs). The coercive field for opposite switching shows a temperature dependency. This affects the proper selection of write/read voltages over the operation temperature range of the device [13]. Of course, the polarization switching kinetics and reliability

properties are highly desirable information for a successful introduction of HfO_2-based ferroelectric thin films in applications.

Thermal stability of the remanent polarization measured at high field levels has been reported for Si:HfO_2 ferroelectric thin films [14]. In this work, we detail the experimental investigation of temperature dependent polarization hysteresis behavior measured over a wide applied field range from 0.5 to 4.0 MV/cm for the same composition. In addition, the switching endurance properties were studied preliminarily at various bipolar stressing fields. The results are of huge technical importance for optimizing device operation conditions, as well as are scientifically interesting for the understanding of domain switching dynamics.

2. Experimental techniques

Metal-ferroelectric-metal (MFM) planar capacitor structures consisting of Pt (50 nm) /TiN (10 nm)/Si:HfO_2 (10 nm)/TiN (10 nm) film stack were grown onto silicon substrates. In detail, the TiN electrodes were formed by atomic layer deposition (ALD) using $TiCl_4$ and NH_3 precursors at 450 °C. The Si:HfO_2 thin films were grown by ALD at 280 °C with $Hf[N(CH_3)C_2H_5]_4$ (TEMAH) and $Si[N(CH_3)_2]_4$ (4DMAS) as precursors, and ozone (O_3) was used as an oxygen source. Sub-cycles of 4DMAS during HfO_2 deposition resulted in a silicon dopant content of ~5.0 mol. %. Crystallization of the Si:HfO_2 films was induced by a 800 °C/20s RTP anneal in N_2 after top TiN electrode deposition. Evaporated platinum dots with radius ranging from 55 μm to 225 μm served as electrical contacts and as a hard mask in chemical etching of the top TiN layer.

Janis ST-500 probe station was used for electrical probing of the capacitor array with the Pt dots (100 μm radius) being stressed and the common bottom TiN electrode being grounded. The polarization-electric field (*P-E*) hysteresis curves and endurance properties were characterized using an aixACCT TF Analyzer 2000 system. For *P-E* hysteresis measurements in a wide temperature range from 100 K to 400 K, the triangular waveform electric field was applied at a frequency of 1.0 kHz, and the maximum field amplitudes (E_{max}) were varied from 0.5 to 4.0 MV/cm. Before the measurements presented in this work, each capacitor was first subjected to a ± 3.0 MV/cm bipolar high field cycling at a frequency of 1.0 kHz for 5 s. Such a "wake-up" or de-ageing treatment was dedicated to minimize the asymmetry and distortion of the polarization hysteresis loop [15].

3. Results and discussion

3.1. Electric field and temperature scaling of polarization hysteresis

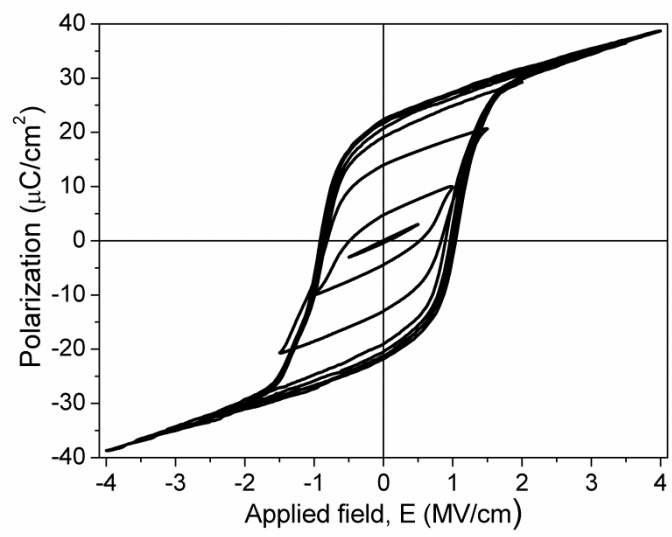

Fig. 1. Evolution of *P-E* hysteresis loops with increasing external applied field amplitude. The measurements were performed at room temperature and 1.0 kHz.

Fig. 1 shows the polarization hysteresis loops measured at room temperature (RT), from which three categories of polarization reversal behavior can be identified depending on the amplitude of the applied field.

Well-saturated *P-E* loops can be obtained in the high-field region ($E_{max} \geq 2.0$ MV/cm), where an increasing field amplitude causes only very slight increases in the remanent polarization (P_r) and coercive field (E_c). At E_{max} = 4.0 MV/cm, the measurement gives a $2P_r$ ($2P_r = P_r^+ - P_r^-$) of ~43.7 μC/cm^2 and an average coercive field ($(E_c^+ - E_c^-)/2$) of ~1.0 MV/cm. In contrast to PZT films, which are normally thicker than 70 nm in integrated ferroelectric memory products, the $2P_r$ value of our 10 nm thick Si:HfO_2 thin films is comparable (30 – 45 μC/cm^2 for PZT), but the coercive field is roughly one order of magnitude higher [13, 16]. The Si:HfO_2 thin film can withstand extremely high electric field strength mainly due to its relatively low dielectric constant, and therefore lower local electric-field that distorts and weakens the molecular bond [17].

In the medium-field regime ($E_c \leq E_{max} < 2\ E_c$), minor loops resulting from partial switching of domains in the material can be observed. The portion of switched domains, which is represented by the remanent polarization and loop area, is very sensitive to the field amplitude applied in this regime. For PZT films used FeRAM application, the write operation requires twofold coercive voltage ($2V_c$) to ensure sufficient and stable nonvolatile switching charge that can be read by subsequent applied voltage pulse [13]. Our measurements show that the same conclusion applies to the use of Si:HfO_2

ferroelectric thin films in FeRAM. When the applied field is further reduced into the low-field region ($E_{max} < E_c$), almost linear *P-E* curve can be seen in Fig. 1. The slope represents the dielectric permittivity at zero field.

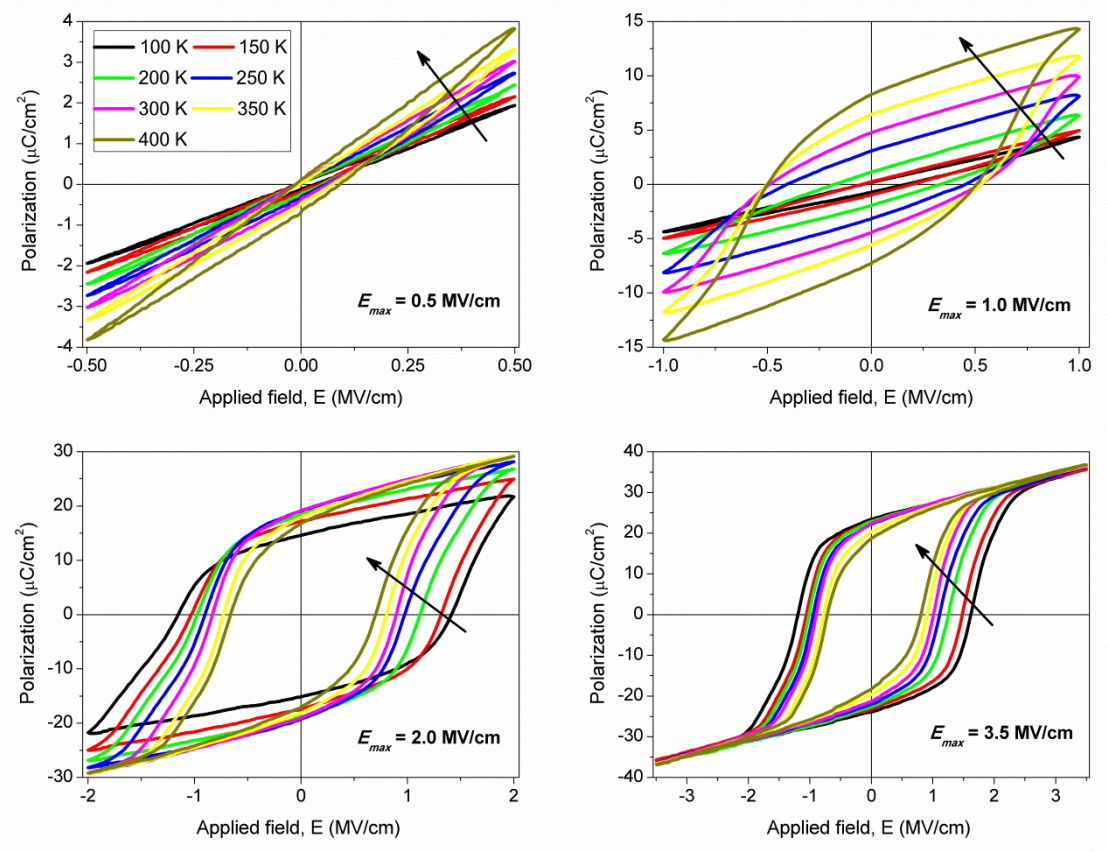

Fig. 2. Temperature dependent *P-E* loops measured at maximum electric fields of 0.5, 1.0, 2.0 and 3.5 MV/cm. The arrows in the figures indicate the evolution trend of the *P-E* loops with increasing temperature.

Fig. 2 displays temperature dependent *P-E* loops measured at E_{max} = 0.5, 1.0, 2.0 and 3.5 MV/cm, which were selected as representative applied fields in aforementioned low-, medium-, and high-field regions. It is demonstrated that, depending on the field regions where the measurements were performed in, temperature scaling of the polarization hystereses differs significantly in terms of the area, shape, and remanent

polarization as well as coercive field. The evolution of the latter two characteristic parameters was depicted in Fig. 3. In subsections 3.2 and 3.3, we summarize the main experimental findings in three measured field regions, and discuss the mechanisms underlying the differences in thermal effects on polarization reversal behavior.

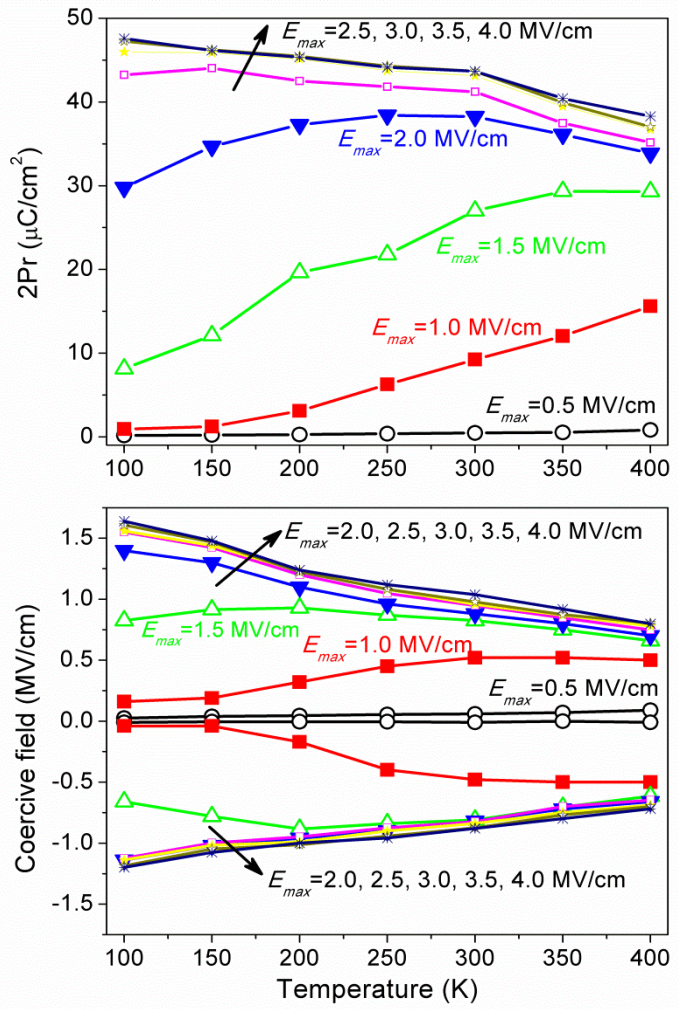

Fig. 3. Temperature dependent remanent polarization and coercive field measured at maximum field amplitudes (E_{max}) from 0.5 up to 4.0 MV/cm.

3.2. Kinetics of polarization reversal in low ($E_{max} < E_c$) *and medium* ($E_c \leq E_{max} < 2\ E_c$) *electric field regimes*

When measured in low-field region, irreversible domain-wall displacement is

regarded as the main source of the weak hysteresis observed in *P-E* curves. In such a non-switching condition, the domain structure on average remains the same, while a low electric field will cause large scale translation of existing domain walls across periodic potential wells created by an array of pining defects [10, 18]. Contribution of domain-wall displacement to the electromechanical properties has been studied intensively for $BaTiO_3$ and PZT ceramics, which the dielectric and piezoelectric non-linearity and hysteresis can be well described by the Rayleigh relations [19, 20]. It is evident that，at E_{max} = 0.5 MV/cm shown in Fig. 2，the hysteresis area and average gradient of the *P-E* loops increase with increasing temperature, giving increases in the energy dissipation and effective permittivity($\varepsilon_r \approx 44$ at 100K and $\varepsilon_r \approx 86$ at 400K). Similar temperature dependence of the Rayleigh-like hysteresis has been reported for PZT thin films, and the underlying mechanism was attributed to widening of the domain wall and resultant weakening of the pining force with increasing temperature [18]. Detailed study on the Rayleigh behavior in Si:HfO_2 ferroelectric thin films will be reported in a subsequent paper.

At medium-field levels close to the coercive field, partial domain switching will be induced, resulting in unsaturated polarization hysteresis loops seen e.g. at E_{max} =1.0 MV/cm in Fig. 2. For ferroelectric Si:HfO_2 thin films, the polarization reversal dynamics have been investigated using pulse switching tests at RT. At relatively low fields, the switching process was found to be very slow, with a steady increase of the switched polarization continuing over many time decades [14, 21]. The experimental

evidence suggests that the switching process follows the nucleation-limited-switching (NLS) mechanism proposed by Tagantsev *et al* [22]. The NLS model considers the polycrystalline film as an ensemble of microscopic regions having independent switching kinetics, and explains retardation of the switching by a wide distribution of nucleation time at these regions. Further work by Jo *et al.* found that the logarithmic switching times obeyed the Lorentzian distribution arising from local field variations due to randomly distributed domain-pinning defects [23].

Taking the concepts of independently switched regions and local field variations, the temperature dependent *P-E* hysteresis measured in medium-field region may be interpreted as following. For each region, domain nucleation can be activated only if the local driving field reaches a certain critical level to effectively surmount the energy potential barrier separating two opposite polarization states. The critical nucleation field differs from region to region; while in general, increases in both external applied field and temperature can facilitate it to be achieved. The latter is related to the thermal-activation mechanism [24, 25]. At very low temperatures (e.g. 100 K and 150 K), a rather high critical nucleation field is needed to surmount almost completely the energy barrier. Fig. 2 shows that such a switching condition could be satisfied at hardly any regions for the case of E_{max} = 1.0 MV/cm, and therefore the *P-E* curves still exhibit Rayleigh-like hysteresis. At elevated temperatures from 150 K to 400 K, the thermal energy promotes domain nucleation at more and more regions resulting in the measured switched polarization increasing accordingly.

In contrast to the thermal energy, the strength of the external applied field plays a more decisive role to trigger domain nucleation. As seen in Fig. 3, even at 100 K, an external field of 1.5 MV/cm can induce noticeable polarization switching. The $2P_r - T$ relationships recorded at 1.0, 1.5 and 2.0 MV/cm indicate further that there exists an upper limit for the achievable number of nucleated regions at a certain medium-field level. An increase in field amplitude causes a raise of the upper limit and accomplishment of it at lower temperatures. After such an upper limit being reached, the switched polarization decreases with increasing temperature. As experimentally confirmed in subsection 3.3, this should be attributed to a reduction of the spontaneous polarization.

Apart from aforementioned nucleation mechanisms, the kinetics of domain wall motion should also to be taken into account in consideration of the total polarization reversal process. The polycrystalline film contains lots of impurities and defects acting as pining sites for widening of the switched domains. As demonstrated by experimental and theoretical studies, a so-called domain wall creep motion can occur at relatively low applied fields [23, 26, 27]. The velocity of domain wall motion increases exponentially with increasing field and temperature, yielding faster completion of switching in independent regions, and therefore more irreversible polarization switching within the measuring time.

3.3. Kinetics of polarization reversal in high-field regime ($E_{max} \geq 2E_c$)

If the external applied field is much higher than the coercive field (E_{max} > 2.0

MV/cm in our case), the time taken for domain wall expansion and distribution of local fields can be neglected. Based on these assumptions, Vopsaroiu *et al.* introduced the classical Landau-Devonshire free energy functions in their non-equilibrium statistical model, which can predict the effects of temperature, time and electric field on polarization switching dynamics successfully [28]. For all independent switching regions (defined as elementary polar sites by the authors), the nucleation process is considered to be activated when the region of reversed polarization reaches a critical volume V^*. The reversal time of the material is determined by the switching rate of the critical volume V^*. At higher temperatures, the reversal time is much faster, as the increased thermal energy makes the transition over the energy barrier more probable. For our measurements with fixed electric field ramping rate (i.e., fixed frequency), this effect is represented by a reduction of the coercive field with increasing temperature.

Vopsaroiu's model derives an analytical expression for the time and thermal dependence of the coercive field,

$$E_c(t, T) \cong \frac{W_B}{P_s} - \frac{k_B T}{V^* P_s} . ln\left(\frac{v_0 t}{ln(2)}\right), \quad (1)$$

where W_B is the energy barrier per unit volume, P_s is the spontaneous polarization, k_B = 8.62×10^{-5} eV/K is the Boltzmann constant, v_0 is a constant equal to the total number of trials per second to overcome the energy barrier, T is the measurement temperature, and t is the time taken to reach the E_c. Assuming W_B and P_s are constants, Eq. (1) predicts a linear relationship between the E_c and measuring temperature.

For the *P-E* loops acquired at E_{max} = 3.0 MV/cm and f = 1.0 kHz, the values of

averaged coercive field ($(E_c^+ - E_c^-)/2$) have been extracted and plotted as a function of the measuring temperature. As shown in Fig. 4, the $E_c - T$ plot represents a fairly good fit to a linear relationship, indicating the applicability of Eq. (1) in certain measuring frequency and temperature ranges.

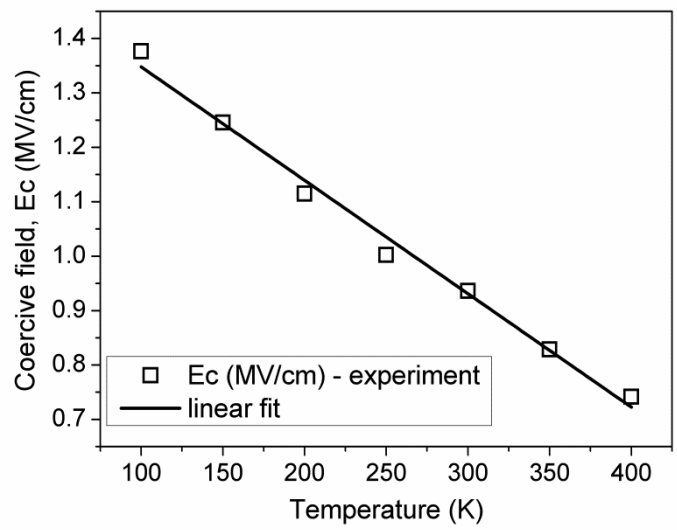

Fig. 4. Coercive field versus temperature from *P-E* loops measured at 1.0 kHz and E_{max} = 3.0 MV/cm.

The linear fit gives an intercept of 1.56 × 10^8 V/m and a slope of –2.08 × 10^5 V/(m.K). Referring to the first principles study for ferroelectric Si:HfO_2 [4], we introduce P_s = 0.41 C/m^2 and the soft mode attempt frequency ν_0 = 1.16 × 10^{13} Hz. The time taken to reach the E_c is approximated as t =0.001/8 s (frequency 1.0 kHz).Then using Eq. (1), we calculated that the nucleation activation volume (V*) and its corresponding energy barrier ($W_B \times V$*) were 3.47 × 10^{-27} m^3 and 1.38 eV, respectively. Note that the calculated V* is two orders of magnitude lower than that of soft PZT ceramics [29]. While, if assuming sphere shape of the polar nucleation site, the radius of the nucleation activation volume V* is given by,

$$r = \sqrt[3]{3V^*/4\pi}. \quad (2)$$

The result of r = 0.94 nm is quite reasonable for our thin film sample of 10 nm thickness.

As shown in Fig. 3, the $2P_r$ value measured at high-field levels decreases apparently with increasing temperature. However, the polarization recorded in full saturation segment of the *P*-*E* curve is almost identical in a wide temperature range, and even increases slightly at 400 K (see the example of E_{max} = 3.5 MV/cm in Fig. 2). In order to explain these phenomena, the so-called Positive-Up-Negative-Down (PUND) test was performed. The principle of PUND test specified by the aixACCT TF Analyzer 2000 system is depicted in Fig. 5a-c. Upon application of the Up pulse with polarity as same as that of the Preset pulse, the electric displacement response contains mainly the leakage current and dielectric capacitance contributions, which form the positive non-switching half loop (the initial value has been zeroed for illustration and subsequent calculation). The Positive pulse is used to fully align domains (all being preseted in negative direction by the Negative and Down pulses) positive direction, the total polarization response is a summation of the ferroelectric domain-switching and the non-switching components. The two positive polarity measurement curves are subtracted from each other (*Positive* - *Up*) to produce a half *P*–*E* loop for $E > 0$, which represents the variation of *pure* ferroelectric polarization due to domain-switching from negative to positive direction. Repeating this procedure using Negative and Down pulses, a closed PUND hysteresis loop can be obtained. Note that, for all pulses, a slight

amount of polarization relaxation can be observed at zero field. This should be resulted from back-switching of a small quantity of domains during delay (5 s in this work) between pulses.

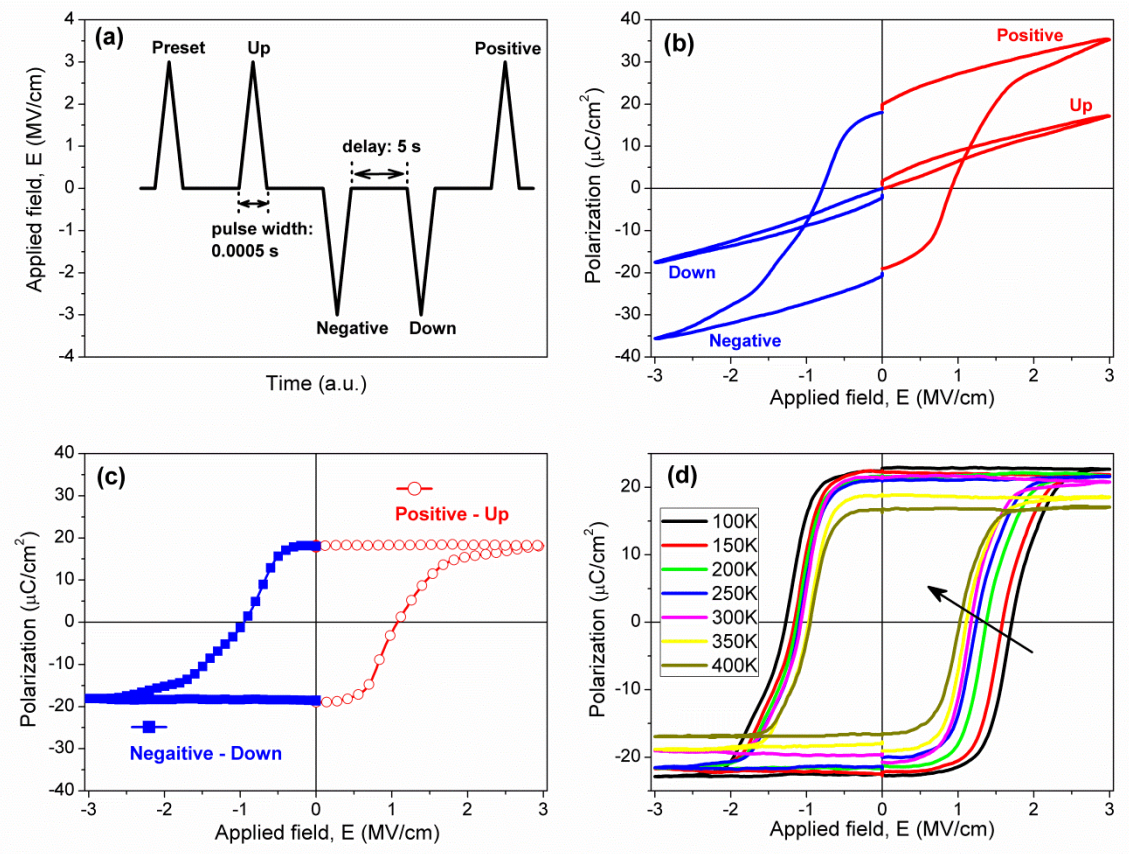

Fig. 5. (a) Schematic illustration of electric field pulses used in PUND test. (b) Example of *P*-*E* curves obtained from Positive, Up, Negative and Down pulses. (c) Example of a closed PUND hysteresis loop produced by subtracting Up (Down) curve from Positive (Negative) curve. (d) PUND hysteresis loops recorded at E_{max} = 3.0 MV/cm and different temperatures.

Fig. 5d shows the temperature dependency of PUND hysteresis loops measured at Emax = 3.0 MV/cm. It is clear that the saturation polarization decreases with increasing temperature. This should be mainly attributed to a reduction of the spontaneous polarization (P_s) as predicted by the Landau-Devonshire thermodynamic theory [28]. The dielectric capacitance and conduction current characteristics of Si:HfO2

ferroelectric thin films have been investigated in our previous work, and it was shown that these two non-switching components increased with increasing temperature [17]. Therefore a competition between reduction of P_s and increases in non-switching components can explain the contradictory observation of temperature dependent remanent and saturation polarization recorded by conventional *P-E* measurements at high-field levels.

3.4. Endurance characteristics

In addition to the temperature stability of appropriate remanent polarization, fatigue, imprint and retention loss properties are of serious reliability concerns in evaluating the suitability of a ferroelectric material for memory applications. In present work, the bipolar endurance characteristics of Si:HfO_2 ferroelectric thin films have been measured at room temperature. After measuring an initial *P-E* hysteresis, the MIM capacitor was subjected to bipolar rectangular-wave field pulses at a fixed frequency of 100 kHz. The changes of hysteresis shape, remanent polarization, and coercive field invoked by cyclic switching were monitored periodically by dynamic *P-E* measurements using triangular waves, the field amplitude of which was preset as same as the cycling pulses, and the frequency is 1.0 kHz.

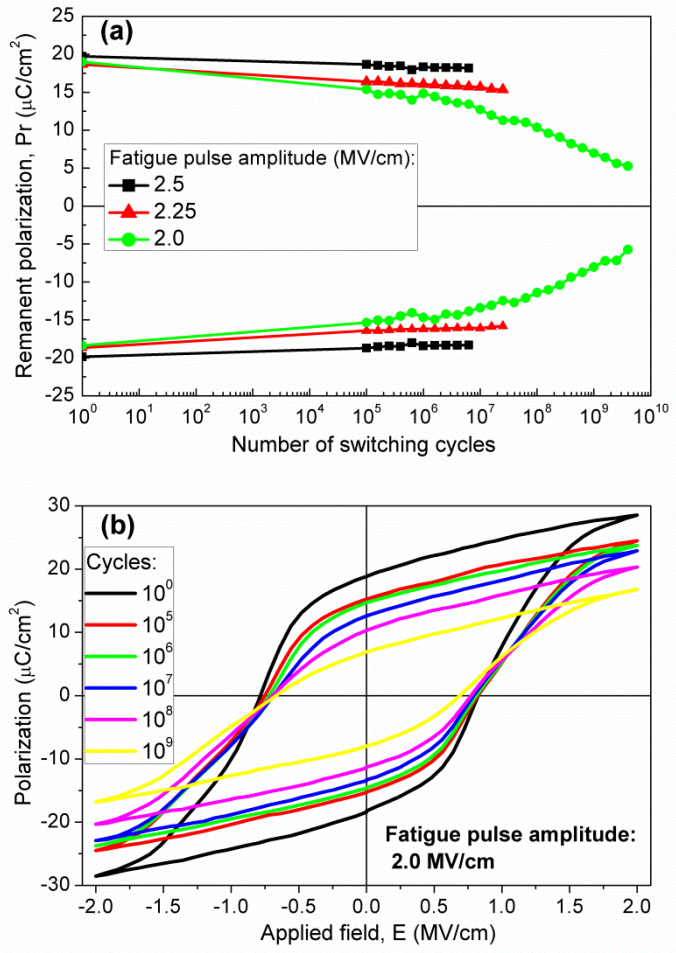

Fig. 6. Endurance characteristics of ferroelectric Si:HfO_2 MIM capacitors measured at room temperature and a bipolar cycling frequency of 100 kHz: (a) the remanent polarization as a function of cycle number for fatigue stressing fields of 2.0, 2.25, and 2.5 MV/cm; (b) evolution of *P*–*E* hysteresis fatigued and measured at an applied field amplitude of 2.0 MV/cm after 1 to 10^9 cycles.

Fig. 6a shows the remanent polarization (P_r) as a function of the number of accumulative switching cycles. A slow decay in P_r can be observed under 2.25 and 2.5 MV/cm bipolar cycling, and the measurements were terminated by breakdown of the ferroelectric layer at about 2.5×10^7 and 6.3×10^6 cycles, respectively. At 2.0 MV/cm, an apparent decrease in P_r starts from 10^6 cycles. Around 30% of the original P_r value (18.7 μC/cm^2) can be held after being fatigued up to 4×10^9 cycles without breakdown.

In the work of Mueller et al [30], endurance up to 10^{10} cycles has been demonstrated at the same bipolar field amplitude. In Fig. 6b, degradation of the hysteresis shape, P_r and E_c can be perceived directly through the evolution of *P*-*E* loops with increasing number of fatigue cycles. Our endurance test results indicate that improvement of the resistances to breakdown and fatigue is a task of high priority for a successful introduction of HfO_2-based ferroelectric thin films into commercial memory devices. There is no doubt that experiences learned from the developments of high-*k* and perovskite-type ferroelectric materials will facilitate the early fulfillment of this task.

4. Conclusions

In summary, temperature and field dependent polarization hysteresis behavior have been investigated for Si:HfO_2 ferroelectric thin films. In the low-to-medium-field regime, the widening of non-switching and sub-switching hysteresis with increasing temperature was mainly attributed to thermally activated domain-wall motion and domain nucleation at increasing number of regions, respectively. In the high-field regime, the increased thermal energy facilitates faster switching, and therefore a decrease in coercive field with increasing temperature was observed. For memory device applications, we recommend an operation field in the vicinity of 2.0 MV/cm (i.e. 2.0 V across 10 nm thick films), whereby the remanent polarization is sufficient and exhibits a good temperature stability. Additionally, endurance without breakdown up to 4×10^9 cycles has been demonstrated at this field level.

Acknowledgements

Work of the authors in China was supported by the National Natural Science Foundation of China (Grant No. NSFC 51272034) and the Open Research Fund of State Key Laboratory of Electronic Thin Films and Integrated Devices (UESTC) (No. KFJJ201101). Authors in Germany were financially supported by the Free State of Saxony (CoolMemory Project).

References

[1] U. Schroeder, E. Yurchuk, J. Müller, D. Martin, T. Schenk, P. Polakowski, C. Adelmann, M.I. Popovici, S.V. Kalinin, T. Mikolajick, Jpn J Appl Phys 53 (2014) 08LE02.

[2] J. Müller, T. S. Böscke, U. Schröder, S. Mueller, D. Bräuhaus, U. Böttger, L. Frey, T. Mikolajick, Nano Lett 12 (2012) 4318-4323.

[3] D. Martin, J. Müller, T. Schenk, T.M. Arruda, A. Kumar, E. Strelcov, E. Yurchuk, S. Müller, D. Pohl, U. Schröder, S.V. Kalinin, T. Mikolajick, Adv Mater 26 (2014) 8198-8202.

[4] S. Clima, D.J. Wouters, C. Adelmann, T. Schenk, U. Schroeder, M. Jurczak, G. Pourtois, Appl Phys Lett 104 (2014) 092906.

[5] T.D. Huan, V. Sharma, G.A. Rossetti, Jr., R. Ramprasad, Phys Rev B 90 (2014) 064111.

[6] S.E. Reyes-Lillo, K.F. Garrity, K.M. Rabe, Phys Rev B 90 (2014) 140103(R).

[7] International Technology Roadmap for Semiconductors-Emerging Research Devices, 2013 edition.

[8] J. Müller, E. Yurchuk, T. Schlösser, J. Paul, R. Hoffmann, S. Müller, D. Martin, S. Slesazeck, P. Polakowski, J. Sundqvist, M. Czernohorsky, K. Seidel, P. Kücher, R. Boschke, M. Trentzsch, K. Gebauer, U. Schröder, T. Mikolajick, in Proceedings of the VLSI Technology Symposium (2012), pp. 25–26.

[9] N. Setter, D. Damjanovic, L. Eng, G. Fox, S. Gevorgian, S. Hong, A. Kingon, H. Kohlstedt, N.Y. Park, G.B. Stephenson, I. Stolitchnov, A.K. Taganstev, D.V. Taylor, T. Yamada, S. Streiffer, J Appl Phys 100 (2006) 051606.

[10] D. Damjanovic, Rep Prog Phys 61 (1998) 1267-1324.

[11] A.K. Tagantsev, I. Stolichnov, E.L. Colla, N. Setter, J Appl Phys 90 (2001) 1387-1402.

[12] C.A-Paz de Araujo, J.D. Cuchiaro, L.D. McMillan, M.C. Scott, J.F. Scott, Nature 374 (1995) 627-629.

[13] S. Kawashima, J.S. Cross, FeRAM, Chap. 8 in: K. Zhang(Eds.), Embedded Memories for Nano Scale VLSIs, Springer, New York, 2009, pp.285-291.

[14] U. Schroeder, S. Mueller, J. Mueller, E. Yurchuk, D. Martin, C. Adelmann, T. Schloesser, R. van Bentum, T. Mikolajick，ECS J Solid State Sci Technol 2 (2013) N69-N72.

[15] D. Zhou, J. Xu, Q. Li, Y. Guan, F. Cao, X. Dong, J. Müller, T. Schenk, U. Schröder, Appl Phys Lett 103 (2013) 192904.

[16] K. Kim, S. Lee, J Appl Phys 100 (2006) 051604.

[17] D. Zhou, J. Müller, J. Xu, S. Knebel, D. Bräuhaus, U. Schröder, Appl Phys Lett 100 (2012) 082905.

[18] D. Damjanovic, Hysteresis in Piezoelectric and Ferroelectric Materials, Chap.4 in: I. Mayergoyz and G. Bertotti (Eds.),The Science of Hysteresis, Elsevier, 2005, pp.337-465.

[19] D.A. Hall, P.J. Stevenson, Ferroelectrics 228 (1999) 139-158.

[20] D. Damjanovic, M. Demartin, J Phys D Appl Phys 29 (1996) 2057-2060.

[21] S. Mueller, S.R. Summerfelt, J. Müller, U. Schroeder, T. Mikolajick, IEEE Electron Device Lett 33 (2012) 1300-1302.

[22] A.K. Tagantsev, I. Stolichnov, N. Setter, Phys Rev B 66 (2002) 214109.

[23] J.Y. Jo, H.S. Han, J.G. Yoon, T.K. Song, S.H. Kim, T.W. Noh, Phys Rev Lett 99 (2007) 267602.

[24] I. Stolichnov, A. Tagantsev, N. Setter, J.S. Cross, M. Tsukada, Appl Phys Lett 83 (2003) 3362-3364.

[25] K.B. Chong, F. Guiu, M.J. Reecea, J Appl Phys 103 (2008) 014101.

[26] T. Tybell, P. Paruch, T. Giamarchi, J.-M. Triscone，Phys Rev Lett 89 (2002) 097601.

[27] J.Y. Jo, S.M. Yang, T.H. Kim, H.N. Lee, J.-G. Yoon, S. Park, Y. Jo, M.H. Jung, T. W. Noh, Phys Rev Lett 102 (2009) 045701.

[28] M. Vopsaroiu, J. Blackburn, M.G. Cain, P.M. Weaver, Phys Rev B 82 (2010)

024109.

[29] M. Vopsaroiu, P.M. Weaver, M.G. Cain, M.J. Reece, K.B. Chong, IEEE Trans Ultrason Ferroelect Freq Contr 58 (2011) 1867-1873.

[30] S. Mueller, J. Müller, U. Schroeder, T. Mikolajick, IEEE Trans Device Mater Reliab 13 (2013) 93-97.